9th IFAC Symposium on Nonlinear Control Systems
The International Federation of Automatic Control
September 4-6, 2013. Toulouse, France

Collision Avoidance in Formation Control using Discontinuous Vector Fields

E.G. Hernandez-Martinez * **E. Aranda-Bricaire** **

* *Engineering Department, Universidad Iberoamericana, 01219, Mexico DF, Mexico (e-mail: eduardo.gamaliel@ibero.mx).*
** *Electrical Engineering Department, CINVESTAV, AP 14-740, 7000 Mexico DF, Mexico (e-mail: earanda@cinvestav.mx).*

Abstract: This paper presents a novel collision avoidance approach in formation control for Multi-agent Robots. The control strategy consists in the mix of attractive vector fields and repulsive vector fields based on a scaled unstable focus centered at the position of another robot, instead of the vector fields obtained from the negative gradient of repulsive potential functions. The analysis of the closed-loop system is presented for the case of two point robots. After that, a modification of the composite vector field is proposed adding a discontinuity in order to avoid the undesired equilibria of the system. Real-time experiments using unicycle-type robots show that the control strategy exhibits good performance.

Keywords: Mobile robots; Formation Control; Collision Avoidance; Variable Structure control.

1. INTRODUCTION

Formation control is a current research area of motion coordination for Multi-agent Robots Systems [Arai et al, 2002]. The goal is to coordinate a group of mobile agents to achieve a particular geometric pattern. The range of applications of formation strategies includes toxic residues cleaning, transportation and manipulation of large objects, alertness and exploration, searching and rescue tasks and simulation of biological entities behaviors [Chen and Wang, 2005, Desai et al, 2001]. The main feature of the formation strategies is the decentralization of the control laws because it is assumed that every robot knows the position of certain team members only and, eventually, it senses the position of other robots when a minimal allowed distance is violated to avoid collisions [Lin et al, 2004, Balch and Arkin, 1998, Cao et al, 1997]. Decentralized schemes also allow less computational charge in the local controllers of the robots and scalability to large groups.

The formation strategies were initially based on vector fields obtained as the negative gradient of an artificial potential function, applied to the case of one mobile robot [Rimon and Koditschek, 1992]. This function is composed by the sum of an Attractive Potential Function (APF), centered in the position of an static goal, and the eventual smooth appearance of a local Repulsive Potential Function (RPF) placed in the proximity of a fixed obstacle [Leonard and Fiorelli, 2001, Tanner and Kumar, 2005]. The extension of the mix of APF's and RPF's to the case of multi-robot formation involves the sum of local APF now depending of the dynamic positions of other robots and RPF's that appear in the case of a collision danger between a pair of agents. The standard design of a RPF is based on rational functions of the distance of a pair of agents which tends to infinity when the agents collide and vanishes smoothly until the minimal allowed distance is reached [Tanner and Kumar, 2005, Dimarogonas and Kyriakopoulos, 2006]. The most well-known RPF in the literature was designed by Khatib [Rimon and Koditschek, 1992]. The main drawback of the sum of APF and RPF is the appearance of undesired equilibria where the composite vector field vanishes and the robots are trapped at an undesired position. Also, the analysis to calculate these equilibria and the trajectories which do not converge to the desired formation is very complex [Do, 2006]. In Dimarogonas and Kyriakopoulos [2006], it is shown the complexity analysis of decentralized RPF's applied to formations with bidirectional communication. However, the convergence analysis discards the undesired equilibria.

In the literature, some approaches have been proposed to ensure the convergence and collision avoidance preventing the undesired equilibria. The *navigation functions* approach [Dimarogonas et al, 2006, De Gennaro and Jadbabaie, 2006] design functions with attractive and repulsive behavior to eliminate the undesired equilibria. The drawback is that the non-collision strategy loses decentralization because it requires full-knowledge of the system. Also, most of these functions are high-order with a corresponding high computational cost for the real-time implementation. On the other hand, some approaches propose small perturbations to allow the agents to escape from these equilibria [Antich and Ortiz, 2005, Ge and Fua, 2005]. However, the previous strategies do not include formal proofs about the convergence to the desired formation. Finally, the use of non-smooth vector fields can rule out the existence of undesired equilibria. Some works about discontinuous vector fields in formation control are Yao et al [2006], Loizou et al [2003], Hernandez-Martinez and Aranda-Bricaire [2009]. The analysis falls on the control of variable structure systems [Itkis, 1976, Filippov, 1988]. In most works, the repulsive discontinuous forces are designed heuristically and no formal proofs are presented, for instance [Barnes et al, 2007].

In this paper, a novel decentralized non-collision strategy is presented. The repulsive force is not obtained as the gradient of any RPF. Instead, the repulsive force is obtained from a vector field based on a scaled unstable focus. The approach is an alternative to the standard methodologies and was announced in Hernandez-Martinez and Aranda-Bricaire [2011]. The analysis is carried out for the case of two point robots and extended to the front point of unicycle-type robots. It is demonstrated that there exists an undesired equilibrium which correspond to a saddle point inside the influence region of the repulsive forces. To rid this equilibrium, a discontinuity of the vector field is forced to ensure that the agents do not cross the minimum distance and therefore, the undesired equilibria is get rid of. Real-time experiments show that the agents trajectories exhibit good performance.

2. PROBLEM STATEMENT AND STANDARD METHODOLOGY

Denote by $N = \{R_1, R_2\}$, a set of two agents moving in plane with positions $z_i(t) = [x_i(t), y_i(t)]^T$, $i = 1, 2$. The kinematic model of each agent or robot R_i is described by

$$\dot{z}_i = u_i, \quad i = 1, 2 \tag{1}$$

where $u_i = [u_{i1}, u_{i2}]^T \in \Re^2$ is the velocity along the X and Y axis of i-th robot. Let $c_{21} = [h_{21}, v_{21}]^T \in \Re^2$ denote a vector which represents the desired relative position of R_1 with respect to R_2 and c_{12} the desired relative position of R_2 with respect to R_1. It is assumed that there are no conflicting interagent objectives, in the sense that $c_{21} = -c_{12}$. Thus, the desired relative position of the two robots is

$$z_1^* = z_2 + c_{21}, \quad z_2^* = z_1 + c_{12} \tag{2}$$

Problem Statement. The control objective is to design a control law $u_i(t)$, $i = 1, 2$, such that $\lim_{t\to\infty}(z_i - z_i^*) = 0$, $i = 1, 2$ and $\|z_1(t) - z_2(t)\| \neq 0$, $\forall t \geq 0$.

Let be d the diameter of a circle that circumscribes each robot. In the rest of the paper, it is considered $d = \|c_{21}\|$ to simplify the computation of the equilibra.

Using the standard methodology of artificial potential functions, for system (1), local APF are defined by

$$\gamma_i = \|z_i - z_i^*\|^2, i = 1, 2 \tag{3}$$

Note that the functions γ_i are positive definite and reach their global minimum ($V_i = 0$) when $z_i = z_i^*$, $i = 1, ..., n$. To avoid collisions between robots, define RPF's given by

$$\psi_i = \delta V_{ij}, i = 1, 2, j = 1, 2, i \neq j \tag{4}$$

where $\delta = \begin{cases} 1, & \text{if} \quad \|z_1 - z_2\|^2 < d^2 \\ 0, & \text{if} \quad \|z_1 - z_2\|^2 \geq d^2 \end{cases}$ and V_{ij} as any function that satisfy $V_{ij} = 0$ and $\frac{\partial V_{ij}}{\partial \beta_{ij}} = 0$ when $\|z_1 - z_2\|^2 = d^2$, V_{ij} is monotonously increasing for $\|z_1 - z_2\|^2 \leq d^2$ and $\lim_{\|z_1 - z_2\|^2 \to 0} V_{ij} = \infty$. The formation control law with collision avoidance is given by

$$u_i = -\nabla(\gamma_i + \psi_i), i = 1, 2 \tag{5}$$

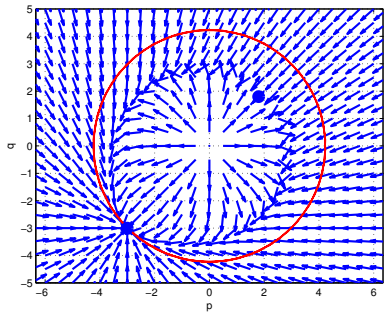

Fig. 1. Standard Khatib's RPF non-collision strategy

A common function V_{ij} reported in the literature was proposed by Khatib [Rimon and Koditschek, 1992] as

$$V_{ij} = \begin{cases} \eta \left(\dfrac{1}{\|z_1 - z_2\|^2} - \dfrac{1}{d^2} \right)^2, & \text{if} \quad \|z_1 - z_2\|^2 \leq d^2 \\ 0, & \text{if} \quad \|z_1 - z_2\|^2 \leq d^2 \end{cases} \tag{6}$$

where $\eta > 0$ is a gain parameter. To study the relative position of agents R_1 and R_2, define the variables

$$p = x_1 - x_2, \quad q = y_1 - y_2 \tag{7}$$

The dynamics of (7) in the closed-loop (1)-(5) is given by

$$\begin{bmatrix} \dot{p} \\ \dot{q} \end{bmatrix} = 2 \begin{bmatrix} -k\,(p - h_{21}) + \delta\eta \dfrac{1}{\tau^2} \left(\dfrac{1}{\tau} - \dfrac{1}{d^2} \right)^2 p \\ -k\,(q - v_{21}) + \delta\eta \dfrac{1}{\tau^2} \left(\dfrac{1}{\tau} - \dfrac{1}{d^2} \right)^2 q \end{bmatrix} \tag{8}$$

where $\tau = p^2 + q^2$. The phase portrait of the system (8) is shown in Figure 1 for $c_{21} = [-3, -3]^T$, $k = 1$ and $\eta = 1000$. Note that there exist an equilibrium in $[-3, -3]$ that corresponds to the desired formation and a undesired equilibrium (saddle point) located within the proximity zone (red circle) when $\delta = 1$. So, the robots will be trapped at the undesired equilibrium point if the initial conditions of robots coincide in the same straight line defined by the goal and the origin of the $p - q$ plane.

3. FORMATION AND NON-COLLISION USING ARTIFICIAL VECTOR FIELDS

As alternative design of the attractive and repulsive forces, let $\varphi_i = -(z_i - z_i^*)$, $i = 1, 2$ be the attractive vector field for every robot. They are stable nodes placed at the desired positions of the robots. It is clear that they can also be seen as the negative gradient of the potential functions (3). Define the repulsive vector fields (RVF's) as

$$\begin{aligned} \beta_1 &= \delta V \begin{bmatrix} (x_1 - x_2) - (y_1 - y_2) \\ (x_1 - x_2) + (y_1 - y_2) \end{bmatrix} \\ \beta_2 &= \delta V \begin{bmatrix} (x_2 - x_1) - (y_2 - y_1) \\ (x_2 - x_1) + (y_2 - y_1) \end{bmatrix} \end{aligned} \tag{9}$$

with δ given in (4) and $V = \left(\frac{d^2}{\|z_1 - z_2\|^2} - 1 \right)$. For each robot, the repulsive vector field is a counterclockwise unstable focus centered at the position of the other robot.

This vector field is scaled by the function V. This function comply with the same features of a RPF. Using these vector fields, we define a new control law given by

$$u_i = k\varphi_i + \eta\beta_i, \quad i = 1, 2 \tag{10}$$

where $k, \eta \in \Re$ and $k, \eta > 0$.

Proposition 1. Consider the system (1) and the control law (10). Suppose that $d = \|c_{21}\|$. Then, in the closed-loop system (1)-(10) there exist two equilibria. The first is a stable node where the agents achieve the desired formation, i.e. $z_i = z_i^*$, $i = 1, 2$. The second is an undesired equilibrium point which appears only when $\delta = 1$ and corresponds to a saddle point.

Proof. The closed-loop system (1)-(10) is given by

$$\dot{z} = (A + B)z + c \tag{11}$$

where $z = [z_1, z_2]^T$, $c = k[c_{21}, c_{12}]^T$,

$$A = k\begin{bmatrix} -1 & 0 & 1 & 0 \\ 0 & -1 & 0 & 1 \\ 1 & 0 & -1 & 0 \\ 0 & 1 & 0 & -1 \end{bmatrix}, B = \delta\eta V \begin{bmatrix} 1 & -1 & -1 & 1 \\ 1 & 1 & -1 & -1 \\ -1 & 1 & 1 & -1 \\ -1 & -1 & 1 & 1 \end{bmatrix}.$$

The dynamics of the variables $[p, q]$ defined in (7) now is given by

$$\begin{bmatrix} \dot{p} \\ \dot{q} \end{bmatrix} = 2\begin{bmatrix} -k\,(p - h_{21}) + \delta\eta V\,(p - q) \\ -k\,(q - v_{21}) + \delta\eta V\,(p + q) \end{bmatrix} \tag{12}$$

where $V = \frac{\|c_{21}\|^2}{\tau} - 1$. For the closed-loop system (12), two cases are to be analyzed. The first case is when $\delta = 0$ where the equilibrium point is given by $p = h_{21}$ $q = v_{21}$, i.e, when $z_i = z_i^* = 0$, $i = 1, 2$. The system matrix of equation (12) with $\delta = 0$ is clearly Hurwitz. Therefore, the agents converge exponentially to the desired position because the equilibria is a stable node. Figure 2 shows a phase plane of this case (outside the red circle) with $c_{21} = [-3, -3]^T$ and $k = 1$ as in the previous case and letting $\eta = 1$.

The second case arises when $\delta = 1$. Now, the equilibria of the system (12) are given by

$$[p_{01}, q_{01}]^T = [h_{21}, v_{21}]^T, \tag{13}$$

$$\begin{bmatrix} p_{02} \\ q_{02} \end{bmatrix} = \begin{bmatrix} -\eta\dfrac{kh_{21} + v_{21}\,(k + 2\eta)}{(k + \eta)^2 + \eta^2} \\ -\eta\dfrac{kv_{21} - h_{21}\,(k + 2\eta)}{(k + \eta)^2 + \eta^2} \end{bmatrix}. \tag{14}$$

The first equilibrium is the same than the previous case where the agents are at the desired position. The distance between agents at the second equilibrium point satisfies

$$p_{02}^2 + q_{02}^2 = \|c_{21}\|^2 \frac{2\eta^2}{(k + \eta)^2 + \eta^2} < d^2 \tag{15}$$

This means that the second equilibrium is an undesired equilibrium which always appears inside the influence zone of the repulsive vector field. The Jacobian matrix J of the system (12) with $\delta = 1$ is computed as

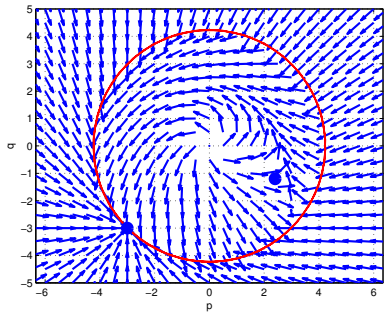

Fig. 2. Phase portrait of the agents with RVF

$$J = 2\begin{bmatrix} -(k + a_1) - b_1 p & a_1 - b_1 q \\ -a_1 - b_2 p & -(k + a_1) - b_2 q \end{bmatrix} \tag{16}$$

where $a_1 = \eta - \frac{\eta\|c_{21}\|^2}{\tau}$, $b_1 = \frac{2\eta\|c_{21}\|^2}{\tau^2}(p - q)$ and $b_2 = \frac{2\eta\|c_{21}\|^2}{\tau^2}(p + q)$. The eigenvalues of the jacobian matrix are given by

$$\lambda_{1,2} = -2\left(k + \eta \pm \eta\sqrt{2\left(\frac{h_{21}^2 + v_{21}^2}{p^2 + q^2}\right)^2 - 1}\right). \tag{17}$$

Evaluating the eigenvalues at the equilibrium point $[p_{01}, q_{01}]$ we obtain $\lambda_1|_{(p_{01},q_{01})} = -2k$, $\lambda_2|_{(p_{01},q_{01})} = -2k - 4\eta$. The eigenvalues at the equilibrium point $[p_{02}, q_{02}]$ are $\lambda_1|_{(p_{02},q_{02})} = -2\,(k + \eta - \eta\xi)$ and $\lambda_2|_{(p_{02},q_{02})} = -2\,(k + \eta + \eta\xi)$ where $\xi = \sqrt{\frac{\left((k+\eta)^2+\eta^2\right)^2}{2\eta^4}} - 1$. In this second case, the behavior of $[p_{01}, q_{01}]$ is a stable node as the first case. The equilibrium point $[p_{02}, q_{02}]$ corresponds to a saddle point because $\lambda_1|_{(p_{02},q_{02})} > 0$ and $\lambda_2|_{(p_{02},q_{02})} < 0$. Therefore, there exists only a single trajectory tending to this undesired equilibrium. ■

Figure 2 shows a phase portrait of this second case (inside the red circle). The calculation of the equilibrium points results in $[p_{01}, q_{01}] = [-3, -3]$ and $[p_{02}, q_{02}] = [2.4, -1.2]$ where $\|p_{02}, q_{02}\|^2 = 7.2 < d^2 = 18$.

4. UNDESIRED EQUILIBRIUM AVOIDANCE

This section presents a strategy to avoid the undesired equilibrium of the closed-loop system (12). Define the influence region of the repulsive forces as

$$M = \{(p, q) | p^2 + q^2 \leq d^2\} \tag{18}$$

Note that the right-hand side of system (12) is differentiable and the boundary ∂M is a compact set. As matter of fact $\partial M = \{(p, q) | \sigma = p^2 + q^2 - d^2 = 0\}$. The quantity $\rho = \max_{(p,q)\in\partial M}(\dot{p}^2 + \dot{q}^2)^{\frac{1}{2}}$ is well defined.

Proposition 2. Consider the system (1) and the control law (10) with $\eta = 1$ and a new function $V = \tilde{V}$ given by $\tilde{V} = \left(\frac{d^2}{\|z_1 - z_2\|^2} - 1\right) + \epsilon$, where $\epsilon \in \Re$, $\epsilon > 0$. Suppose that the initial positions of the agents satisfy $\delta = 0$, i.e. $p(0)^2 + q(0)^2 > d^2$. Then, there exists $\epsilon > \rho$ such that the closed-loop system (1)-(10) exhibits a single equilibrium point which corresponds to the desired formation, i.e. $z_i = z_i^*$, $i = 1, 2$.

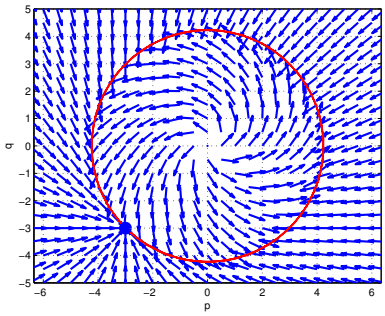

Fig. 3. Phase portrait of the agents with RVF and $\epsilon = 6$

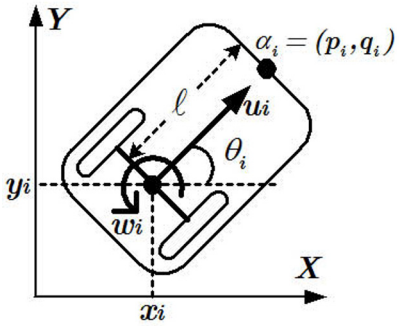

Fig. 4. Kinematic model of unicycles

Sketch of proof. Note that minimum value of $\tilde{V}$ in the surface $\sigma = p^2 + q^2 - d^2 = 0$ is now ϵ and it tends to infinity when the distances between agents tends to zero. Observe that the attractive vector field when $\delta = 0$, points always inside the region M and the repulsive vector field when $\delta = 1$ points always outside the region M. The discontinuity of the composite vector field (10) occurs precisely on the surface $\sigma = 0$. It is always possible to choose an appropriate value of $\epsilon > \rho$, such that the convex hull generated by the attractive and repulsive vector fields contains the tangent space of $\sigma = 0$. Therefore, following [Filippov, 1988, Itkis, 1976] the integrals of the composite vector field slide along the surface $\sigma = 0$. This implies that the trajectories of the closed loop system (1)-(10) reach the equilibrium point (13) which lies on the surface $\sigma = 0$ and corresponds to the desired position of the agents. This concludes the proof. ■

Figure 3 shows the phase portrait of the discontinuous vector fields. The undesired equilibrium point has disappeared and the trajectories never cross the proximity area.

5. EXTENSION TO THE CASE OF UNICYCLE-TYPE ROBOTS AND REAL TIME EXPERIMENTS

In this section, the control laws developed so far are extended to the case of unicycle-type robot formations. The kinematic model of each agent or robot R_i, as shown in Fig. 4 is given by

$$\begin{bmatrix} \dot{x}_i \\ \dot{y}_i \\ \dot{\theta}_i \end{bmatrix} = \begin{bmatrix} \cos\theta_i & 0 \\ \sin\theta_i & 0 \\ 0 & 1 \end{bmatrix} \begin{bmatrix} u_i \\ w_i \end{bmatrix}, \quad i = 1, ..., n \tag{19}$$

where u_i is the linear velocity of the midpoint of the wheels axis and w_i is the angular velocity of the robot. A celebrated result by Brockett [1983] states that the dynamical system (19) can not be stabilized by continuous and time-invariant control law. Because of this restriction, we will analyze the dynamics of the coordinates $\alpha_i = (p_i, q_i)$ shown in Fig. 4 instead coordinates (x_i, y_i). The coordinates α_i are given by

$$\alpha_i = \begin{bmatrix} p_i \\ q_i \end{bmatrix} = \begin{bmatrix} x_i + \ell\cos(\theta_i) \\ y_i + \ell\sin(\theta_i) \end{bmatrix}, i = 1, ..., n. \tag{20}$$

The dynamics of (20) is obtained as

$$\dot{\alpha}_i = A_i(\theta_i)\,[u_i, w_i]^T, i = 1, ..., n \tag{21}$$

where the so-called decoupling matrix $A_i(\theta_i) = \begin{bmatrix} \cos\theta_i & -\ell\sin\theta_i \\ \sin\theta_i & \ell\cos\theta_i \end{bmatrix}$ is non-singular. The idea of controlling coordinates α_i instead of the center of the wheels axis is frequently found in the mobile robot literature in order to avoid singularities in the control law [Desai et al, 2001].

Following the formation control strategy with collisions avoidance presented on Section (3), a formation control strategy with non-collision, similar to (10) is defined as

$$\begin{bmatrix} v_i \\ w_i \end{bmatrix} = A_i^{-1}(\theta_i)\left(k\tilde{\varphi}_i + \eta\tilde{\beta}_i\right), i = 1, 2 \tag{22}$$

where $\tilde{\varphi}_i$ and $\tilde{\beta}_i$ are similar to the case of point robots but related to coordinates α_i. The dynamics of the coordinates α_i for the closed-loop system (19)-(22) is given by

$$\dot{\alpha} = (A + B)\alpha + c \tag{23}$$

where $\alpha = [\alpha_1, \alpha_2]^T$, the matrix A, B and vector C are the same than equation (11) with $V = \left(\frac{d^2}{\|\alpha_1 - \alpha_2\|^2} - 1\right) + \epsilon$. It is clear that the dynamics of coordinates α_i is the same than the case of point robots. Thus, the analysis of convergence and non-collision is reduced to the case of point robots presented before.

Remark 1. The control law (22) steers the coordinates α_i to a desired position. However, the angles θ_i remain uncontrolled. These angles do not converge to any specific value. Thus, the control law (22) is to be considered as a formation control without orientation.

The formation control and collision avoidance strategies presented in Section 3 were implemented in an experimental setup consisting of three unicycle-type robots (model: Yujin YSR-A) and a vision system composed by an UNIQ digital video camera (model: UF1000-CL) connected to and ARVOO video processor (model: Leonardo CL). The vision system captures and processes the position of two white circle marks placed on every robot (the marks represent the position of (x_i, y_i) and α_i) at 100 Hz rate. The position and orientation of each robot are obtained using this information. The images are processed in a Pentium4 based PC where the control actions u_i and w_i are also transformed into the desired angular velocities for the robot wheels using the parameters $\ell = 2.8$cm, the radius of the wheels $r = 2.2$cm and the distance between the two wheels $L = 7.12$cm. These commands are sent by a RF module to every robot.

In both experiments, the control signals were normalized to $[\bar{v}_i, \bar{w}_i]^T = \frac{\mu}{\sqrt{\|F_i\|^2+\varepsilon}} A^{-1}(\theta_i) F_i$, $i = 1, 2, 3$ where $\mu = 0.1$, $\varepsilon = 0.0001$ and F_i is the closed loop composite vector field. The normalization has two purposes. Firstly, to avoid actuator saturation for large values of $\|\alpha_i - \alpha_i^*\|$. Secondly, to compensate the adverse effects of friction and actuators' dead zone.

Figure 5 shows an experiment of the control law (22) with $k = 0.2$, $\eta = 1$ and $\epsilon = 0$. The vector of relative positions is given by $c_{21} = [-0.14, -0.14]$ and consequently $d = 0.198m$. The initial conditions (in meters and radians) are given by $[x_{10}, y_{10}, \theta_{10}] = [0.1625, 0.1252, 0.7797]$ and $[x_{20}, y_{20}, \theta_{20}] = [-0.1706, -0.1948, -2.4772]$. Simulation results are dashed lines and experimental results are solid lines. The robots converge to the desired formation avoiding the collision, however the distance between the two robots can be less than d. Figure 5(d) shows the posture of the robots at final instant recorded by the vision system. Note that the front mark of every robot (coordinates α_i) converge to the desired formation.

Figure 6 illustrates a second experiment with the same parameters of Experiment 1 but $\epsilon = 6$. The initial conditions now are given by $[x_{10}, y_{10}, \theta_{10}] = [0.2318, 0.1359, 0.6047]$ and $[x_{20}, y_{20}, \theta_{20}] = [-0.2300, -0.1852, -2.4812]$. The sliding motion produces the typical chattering effect of the actuators, clearly displayed in Figure 6(b). Note that the distance of the robots is always greater than d.

6. CONCLUSION

A novel non-collision strategy for multi-agent robots formation is presented. The approach consists in the design of a repulsive vector field based on a scaled unstable focus instead of obtaining the repulsive forces from the negative gradient of a repulsive potential function. Formal analysis is provided for the case of two point robots. The analysis of the equilibria shows that there exists an undesired equilibrium point where the agents can be trapped and do not achieve the desired formation. Then, it is demonstrated that this equilibrium point can be avoided using a discontinuos vector field which ensures that the agents slide along a suitable surface and do not cross the minimum allowed distance. The approach is an alternative to the classical design of repulsive forces. In further research, the analysis will be extended to the case of any number of robots with different formation graphs.

ACKNOWLEDGEMENTS

The experiments displayed in this paper were achieved during a short visit of the authors to CICESE premises in Ensenada, Mexico. The authors thank Prof. Rafael Kelly and his coworkers for their hospitality.

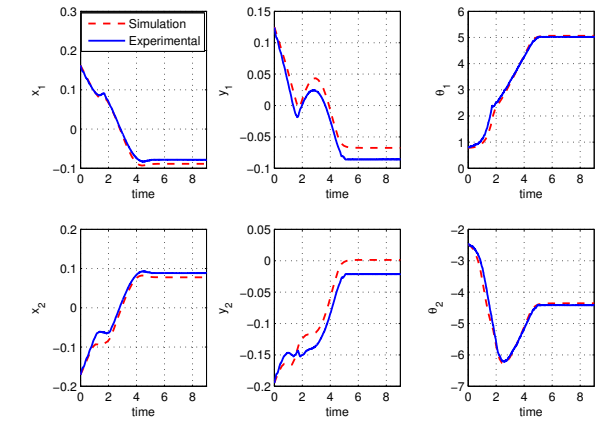

(a) Graphics of x_i, y_i and θ_i,$i = 1, 2$

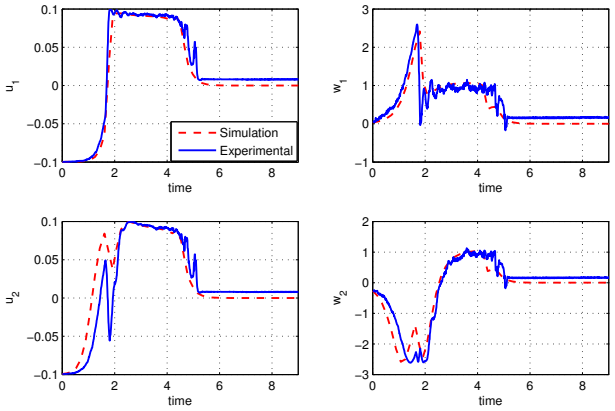

(b) Control inputs

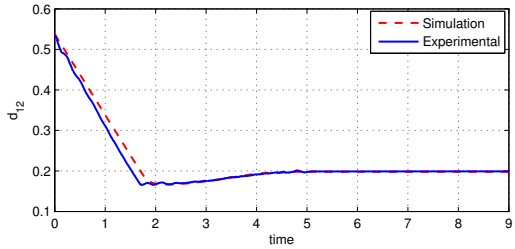

(c) Inter-robot distance

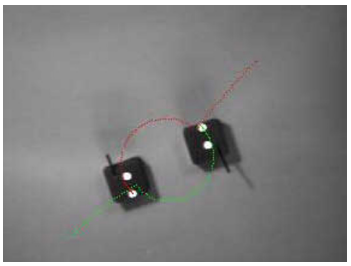

(d) Trajectories of robots in the plane

Fig. 5. Experiment 1 with $\epsilon = 0$

J. Antich, A. Ortiz. Extending the potential fields approach to avoid trapping situations. *IEEE/RSJ IROS*, pages 1386–1391, 2005.

T. Arai, E. Pagello, L.E. Parker. Guest Editorial Advances in Multirobot systems. *IEEE Trans. Robot. Autom.*, 18: 655–661, 2002.

T. Balch, R.C. Arkin. Behavior-based formation control for multirobot teams. *IEEE Trans. Robot. Autom.*, 14: 926–939, 1998.

L. Barnes, M.A. Fields, K. Valavanis. Unmanned ground vehicle swarm formation control using potential

REFERENCES

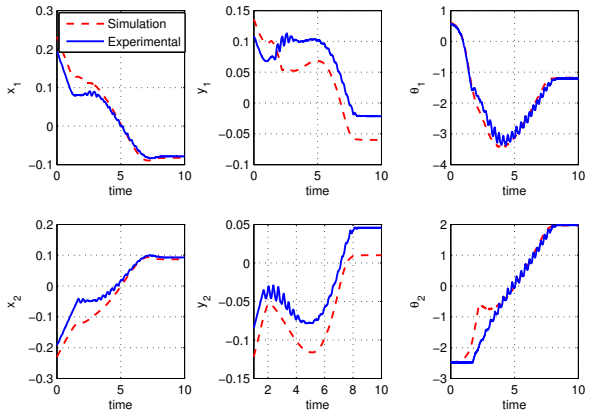

(a) Graphics of x_i, y_i and θ_i,$i = 1, 2$

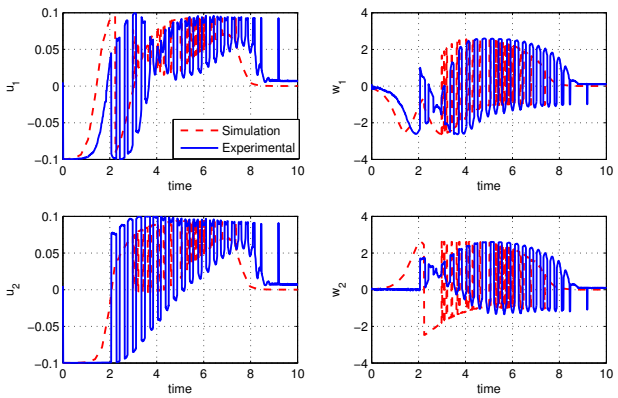

(b) Control inputs

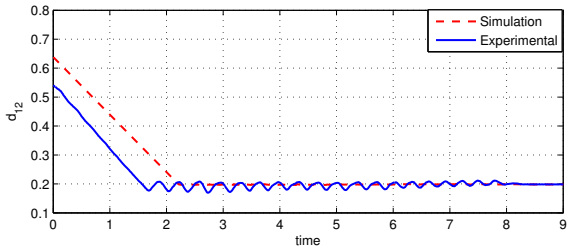

(c) Inter-robot distance

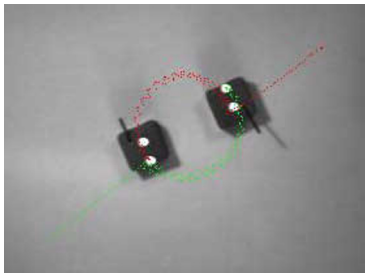

(d) Trajectories of robots in the plane

Fig. 6. Experiment 2 with $\epsilon = 6$

fields. *IEEE Mediterranean Conference on Control and Automation*, pages 1–8, 2007.

R. Brockett. Asymptotic Stability and Feedback Stabilization. In R. Brockett, R.S. Millman, H. J. Sussmann, editors, *Differential Geometric Control Theory*, Birkhauser, Basel-Boston, Massachusetts, 1983.

Y.U. Cao, A.S. Fukunaga, A.B. Kahng. Cooperative mobile robotics: Antecedents and directions. *Autonomous Robots*, 4:34–46, 1997.

Y.Q. Chen, Z. Wang. Formation control: A Review and a New Consideration *IEEE/RSJ IROS*, pages 3181–3186, 2005.

M.C. De Gennaro, A. Jadbabaie. Formation Control for a Cooperative Multi-Agent System using Decentralized Navigation Functions. *ACC*, 2006.

J.P. Desai, J.P Ostrowski, V. Kumar. Modeling and control of formations of nonholonomic mobile robots. *IEEE Trans. Robot. Autom.*, 6:905–908, 2001.

D.V. Dimarogonas, K.J. Kyriakopoulos. Distributed cooperative control and collision avoidance for multiple kinematic agents. *IEEE CDC*, pages 721–726, 2006.

D.V. Dimarogonas, S.G. Loizou, K.J. Kyriakopoulos, M.M. Zavlanos. A feedback stabilization and collision avoidance scheme for multiple independent non-point agents. *Automatica*, 42:229–243, 2006.

K.D. Do. Formation control of mobile agents using local potential functions. *ACC*, pages 2148–2153, 2006.

A.S. Filippov. *Differential Equation with Discontinuous Right-hand Side*. Kluwer Academic Publishers, 1988.

S.S. Ge, C. Fua. Queues and Artificial Potential Trenches for Multirobot Formations. *IEEE Trans. Robot.*, 21: 646–656, 2005.

E.G. Hernandez-Martinez, E. Aranda-Bricaire. Convergence and Collision Avoidance in Formation Control: A survey of the Artificial Potential Functions approach. In F. Alkhateeb, E.A. Maghayreh, I.A. Doush, editors, *Multi-Agent Systems - Modeling, Control, Programming, Simulations and Application*, pages 103–126. INTECH, Austria, 2011.

E.G. Hernandez-Martinez, E. Aranda-Bricaire. Multi-agent formation control with collision avoidance based on discontinuous vector fields. *35th IEEE IECON*, pages 2283–2288, 2009.

U. Itkis. *Control Systems of Variable Structure*. Wiley, 1976.

N.E. Leonard, E. Fiorelli. Virtual Leaders, Artificial Potentials and Coordinated Control of Groups. *IEEE/RSJ IROS*, pages 2968–2973, 2001.

Z. Lin, M. Broucke, B. Francis. Local Control Strategies for Groups of Mobile Autonomous Agents. *IEEE Trans. Autom. Control*, 49:622–629, 2004.

S.G. Loizou, H.G. Tannert, V. Kumar, K.J. Kyriakopoulos. Closed Loop Navigation for Mobile Agents in Dynamic Environments. *IEEE/RSJ IROS*, pages 3769–3774, 2003.

E. Rimon, D.E. Koditschek. Exact Robot Navigation using Artificial Potential Functions. *IEEE Trans. Robot. Autom.*, 5:501–518, 1992.

H.G. Tanner, A. Kumar. Towards Decentralization of Multi-robot Navigation Functions. *IEEE ICRA*, pages 4132–4137, 2005.

J. Yao, R. Ordoñez, V. Gazi. Swarm Tracking Using Artificial Potentials and Sliding Mode Control. *IEEE CDC*, pages 4670–4675, 2006.